

# Caveolae Participate in Tumor Necrosis Factor Receptor 1 Signaling and Internalization in a Human Endothelial Cell Line

Alessio D'Alessio,\* Rafia S. Al-Lamki,<sup>†</sup>  
John R. Bradley,<sup>†</sup> and Jordan S. Pober\*

From the Interdepartmental Program in Vascular Biology and Transplantation,\* Boyer Center for Molecular Medicine, and Department of Pathology, Yale University School of Medicine, New Haven, Connecticut; and the Department of Medicine,<sup>†</sup> University of Cambridge and Addenbrooke's Hospital, Cambridge, United Kingdom

**Caveolae are abundant in endothelial cells (ECs) *in situ* but markedly diminished in cultured cells, making it difficult to assess their role in cytokine signaling. We report here that the human EC line EA.hy926 retains an abundant caveolar system in culture. Tumor necrosis factor (TNF) receptor 1 (TNFR1/CD120a) was enriched in caveolae and co-immunoprecipitated with caveolin-1 from caveolae isolated from these cells. To further investigate the role(s) of caveolae in TNF signaling in ECs, cells were treated with methyl- $\beta$ -cyclodextrin to disrupt caveolae. Methyl- $\beta$ -cyclodextrin did not alter total cell surface expression of TNFR1 or TNF-induced degradation of I $\kappa$ B $\alpha$ , a measure of nuclear factor- $\kappa$ B activation, but it did inhibit TNF-induced phosphorylation of Akt, a measure of phosphatidylinositol-3 kinase activation. Serum-induced phosphorylation of AKT was unaffected. Treatment with TNF induced disappearance of TNFR1 from caveolae and dissociation from caveolin-1 within 5 minutes. In contrast to transferrin receptor, internalized TNFR1 did not co-localize with clathrin, except possibly in the Golgi, at any time point examined. By 60 minutes of treatment with TNF, TNFR1 appeared in endosomes. We conclude that caveolae function in ECs to allow TNFR1 to activate phosphatidylinositol-3 kinase and Akt, perhaps through receptor cross talk, and that ligand-induced internalization and trafficking of TNFR1 to endosomes may originate directly from this compartment. (Am J Pathol 2005, 166:1273–1282)**

Tumor necrosis factor (TNF, sometimes designated TNF- $\alpha$ ) is a pleiotropic cytokine, produced predominantly

by activated macrophages and T lymphocytes,<sup>1</sup> that triggers a broad spectrum of proinflammatory responses.<sup>2,3</sup> Vascular endothelial cells (ECs) are a primary cellular target for TNF actions.<sup>4</sup> Two different surface TNF receptors, TNFR1 (p55-TNFR, CD120a) and TNFR2 (p75-TNFR, CD120b), which independently bind the trimeric TNF molecule with similar affinities, have been identified. Although both receptors are present in cultured human umbilical vein ECs (HUVECs), quiescent ECs *in situ* may express only TNFR1.<sup>5</sup> In culture and *in situ* most TNFR1 molecules in ECs are located in the Golgi apparatus,<sup>5</sup> although only plasmalemmal receptors appear to signal as assessed by ligand-induced recruitment of the cytosolic TNFR-associated death domain (TRADD) adaptor protein.<sup>6</sup> TRADD interacts with the intracytoplasmic death domain of ligand-occupied TNFR1 through its own death domain and receptor-associated TRADD initiates assembly of a multiprotein protein complex (the signalosome) that activates downstream signaling pathways. Specifically, TRADD recruits both TNF-receptor-associated factor 2 (TRAF2) and receptor-interacting protein, leading to nuclear factor (NF)- $\kappa$ B and c-Jun N-terminal kinase activation, and ultimately in transactivation of genes that encode proteins that are proinflammatory and anti-apoptotic/cytoprotective. The signalosome is rapidly internalized and receptor internalization may actually be required for signal initiation by this pathway.<sup>7,8</sup>

Although TNF signaling is initiated by TRADD recruitment at the plasma membrane, it is important to consider that the plasma membrane is not homogenous. Specifically, the plasmalemma typically contains numerous small lipid patches enriched for cholesterol and glycosphingolipids, commonly referred to as lipid rafts. Lipid rafts may function to bring different proteins into proximity and thus promote interactions between receptors and signaling proteins and among different signaling recep-

Supported by the National Institutes of Health (grant HL-36003 and contract HV28286).

Accepted for publication December 20, 2004.

Address reprint requests to Jordan S. Pober, Boyer Center for Molecular Medicine, Room 454, Yale University School of Medicine, 295 Congress Ave., New Haven, CT 06536-0812. E-mail: jordan.pober@yale.edu.

tors.<sup>9</sup> In certain cell types, plasmalemmal lipid rafts can be stably clustered and organized by a scaffolding composed of the intracytoplasmic cholesterol-binding proteins caveolin-1,-2, or (in muscle cells) -3 into 50- to 100-nm flask-shaped invaginations called caveolae. These organelles were originally discovered in the early 1950s by electron microscopic analysis of vascular ECs<sup>10</sup> and of bladder epithelium.<sup>11</sup> Caveolae have since been observed in many cell types although adipocytes, fibroblasts, smooth and striated muscle cells, and ECs show the greatest abundance. Caveolae function to permit transcytosis of macromolecules across an EC barrier such as that found in brain capillaries. More recently, it has been appreciated that caveolae may also play a key role in cell signaling. This is because caveolins, especially caveolin-1, can bind to many types of plasma membrane receptor proteins and concentrate these molecules within the caveolae.<sup>12</sup> This clustering of disparate receptor types further facilitates receptor cross talk, allowing one type of ligand-occupied receptor to activate the downstream signaling pathways normally initiated by a different receptor type.<sup>12,13</sup> In other words, in addition to their role in transcytosis, caveolae appear to function as highly efficient lipid rafts.

The role of caveolae in TNF receptor signaling is primarily unexplored. It has been reported that TNFR1-induced cell death signals originate in caveolae-like domains within a macrophage-like cell type that does not have true caveolae.<sup>14</sup> In cells lacking caveolae, isolated lipid rafts could perform similar functions, albeit with lesser efficiency. It is therefore relevant to note that in several tumor cell lines, which may or may not form caveolae, disruption of lipid rafts by extraction of cholesterol with methyl- $\beta$ -cyclodextrin (M $\beta$ CD) can reduce NF- $\kappa$ B activation.<sup>15</sup> The basis of this effect is not known because the TRADD-activated signaling pathway does not appear to involve other receptors or membrane-bound adaptor proteins. In other words, the proximity effects provided by lipid rafts would not be expected to influence the activation of NF- $\kappa$ B via the signalosome pathway. We and others have shown that TNF treatment can also activate phosphatidylinositol-3 kinase (PI3K)<sup>16-19</sup> and its downstream effector Akt/protein kinase B. In certain cell types, TNF may activate NF- $\kappa$ B by an alternative pathway that involves PI3K and Akt,<sup>20,21</sup> bypassing the signalosome. In cultured HUVECs the activation of PI3K is mediated, at least in part, through TNFR1<sup>17</sup> but the PI3K pathway does not contribute to the activation of NF- $\kappa$ B. It is unknown how TNFR1 actually activates the PI3K pathway, because TNFR1 and PI3K do not appear to interact directly. It has been proposed that TNF may activate PI3K via generation of sphingosine-1 phosphate, presumably acting via a G protein-coupled Edg receptor pathway.<sup>18</sup> Recently, it has been shown that TNF binding to TNFR2 can activate the PI3K pathway in some cells through partial activation of the vascular endothelial growth factor receptor 2, an example of receptor cross talk mediated by the cytosolic enzyme endothelial/epithelial cell tyrosine kinase 1 (Etk-1).<sup>22</sup> We wondered if TNFR1 could also activate PI3K via receptor cross talk, and more specifically, if this process might occur within caveolae (or other lipid rafts) of human ECs. Although HUVECs are the most widely used

model to study EC signaling, they are not appropriate in this case because these cells lose expression of caveolae in a matter of days in culture (A. D'Alessio and J.S. Pober, unpublished observations).<sup>23</sup> We therefore turned to a different model, namely the EA.hy926 cell line, formed by fusion of HUVECs with the human lung carcinoma cell line A549, which retains EC-like responses to TNF, and, as reported here, displays an extensive caveolar system. We show that in this EC line, TNFR1 interacts with caveolin-1 and preferentially localizes to caveolae. Moreover, disruption of caveolae/lipid rafts with M $\beta$ CD inhibits activation of PI3K, but not NF- $\kappa$ B signaling. We also show that TNF causes rapid migration of TNFR1 out of caveolae, eventually concentrating within endosomes without apparent involvement of clathrin-coated pits or vesicles. These results suggest that caveolae may play two distinct roles in TNF signaling in ECs, serving both to foster receptor cross talk (for activation of PI3K) and as a site for initiating ligand-induced receptor internalization.

## Materials and Methods

### Cell Culture

The human-derived EA.hy926 EC line<sup>24</sup> (provided by Dr. W. Sessa, Yale University, New Haven, CT) was maintained in Dulbecco's modified Eagle's medium (Life Technologies, Inc., Gaithersburg, MD) containing 10% (v/v) fetal calf serum, 2% (w/v) hypoxanthine/aminopterin/thymidine (Sigma, St. Louis, MO), 200  $\mu$ mol/L L-glutamine, 100 U/ml penicillin/streptomycin (Life Technologies) at 37°C in a 5% CO<sub>2</sub>-humidified atmosphere. Experiments were performed on cells grown to confluence.

### Reagents and Antibodies

Hypoxanthine/aminopterin/thymidine, MES hydrate, and horseradish peroxidase (HRP) cholera toxin subunit B (CTxB) were from Sigma (St. Louis, MO). Mouse anti-transferrin receptor and Alexa Fluor-conjugated secondary antibodies were all from Molecular Probes (Eugene, OR). Recombinant human TNF- $\alpha$  and goat anti-human TNFR1 antibody were purchased from R&D Systems Inc. (Minneapolis, MN). IgG<sub>2b</sub> mouse anti-TNFR1 (H5) and goat anti-clathrin HC (C-20) antibodies were from Santa Cruz Biotechnology, Inc. (Santa Cruz, CA). Rabbit polyclonal anti-caveolin, mouse monoclonal anti-caveolin-1, anti-EEA1, anti-transferrin receptor, and mouse anti-Rab5 antibodies were from BD Transduction Laboratories (Lexington, KY). Anti-phospho-Akt (Ser473) antibody was from Cell Signaling Technology (Beverly, MA). Horseradish peroxidase goat anti-mouse IgG<sub>2b</sub> antibody was from Southern Biotechnology (Birmingham, AL). Other HRP-conjugated secondary antibodies were from Jackson ImmunoResearch Laboratories (West Grove, PA). Enhanced chemiluminescence was from Pierce (Rockford, IL). All other chemicals were from Sigma. An enzyme-linked immunosorbent assay kit for sTNFR1 was purchased from R&D Systems Inc.

### *Confocal Indirect Immunofluorescence Microscopy*

For immunofluorescence analysis, EA.hy926 cells were grown on 12-mm microscope glass coverslips (Fisher Scientific, Pittsburgh, PA) in 24-well plates. Cells grown to confluence were treated with 10 ng/ml of TNF for the indicated time or left untreated as a control. At the conclusion of the incubation period, free cytokine was removed by washing twice with phosphate-buffered saline (PBS) and cells were fixed with 4% paraformaldehyde for 15 minutes at room temperature and subsequently permeabilized by the addition of 0.2% Triton X-100 for 5 minutes at room temperature. A further blocking step was performed before antibody staining by incubating fixed cells with a buffer containing 1% bovine serum albumin (BSA) and 5% appropriate serum 1 hour at room temperature. Immunostainings were performed by incubating cells with indicated primary antibodies overnight at 4°C in a buffer containing 1% BSA and 5% serum. Detection of bound primary antibody was visualized by the addition of specific Alexa Fluor 488- or 594-conjugated secondary antibodies for 30 minutes at room temperature. For transferrin receptor and caveolin immunostaining the cells were washed with PBS, fixed in 4% paraformaldehyde, and then immunostained as indicated above. All of the images were collected with the Zeiss LSM510 confocal laser-scanning microscopy.

### *Transmission Electron Microscopy*

For transmission electron microscopy, EA.hy926 cells were fixed in 4% formaldehyde, washed three times in 0.1 mol/L PIPES buffer (pH 7.5), postfixated in 1% osmium ferrocyanide in 0.1 mol/L PIPES buffer for 1 hour at room temperature, stained with 2% uranyl acetate, dehydrated in an ascending series of ethanol solutions, and embedded in Spurr's epoxy resin. Sections (40 to 50 nm) were stained with uranyl acetate and lead citrate and viewed in a Phillips CM 100 electron microscope at an accelerating voltage of 80 kV.

### *Immunoelectron Microscopy*

For immunoelectron microscopic examination of sucrose gradient fractions prepared from EA.hy926 cells (see below), samples were absorbed on glow-discharged carbon-coated film grids, excess sample was blotted off on a filter paper and the grids was floated on a small drop (5  $\mu$ l) of blocking buffer consisting of 10% fetal calf serum in 0.1 mol/L Tris-buffered saline, pH 7.5, for 10 minutes at room temperature. Excess blocking buffer was blotted off and the grids were floated on 5  $\mu$ l of mouse monoclonal anti-TNFR1 (1:5 dilution in blocking buffer, 100  $\mu$ g/ml) and rabbit polyclonal anti-caveolin (1:5 dilution in blocking buffer, 50  $\mu$ g/ml) for 30 minutes at room temperature. Grids were then rinsed on several drops of Tris-buffered saline and incubated with 10-nm gold for TNFR1 and 5-nm gold for caveolin (British Biocell, Cardiff, UK) diluted 1:100 for 30 minutes at room temperature. After

several washes in Milli-Q water, grids were negatively stained in 2% phosphotungstic acid, pH 6.8, for 30 seconds and allowed to dry before viewing on a Phillip CM 100 electron microscope at accelerating voltage of 80 kV.

### *M $\beta$ CD Treatments*

To analyze the effects of M $\beta$ CD extraction on cell fractionation, EA.hy926 cells were treated with M $\beta$ CD at 2.5 or 5 mmol/L for 30 minutes, fractionated by sucrose density gradient as described below, and analyzed by sodium dodecyl sulfate (SDS)-polyacrylamide gel electrophoresis (PAGE) and immunoblotting with TNFR1 and caveolin-1 antibodies. To analyze the effects of M $\beta$ CD on cell signaling, EA.hy926 cells, grown on six-well plates, were subjected to serum reduction by incubating in the presence of 0.2% BSA in Dulbecco's modified Eagle's medium containing 2% (w/v), hypoxanthine/aminopterin/thymidine, 200  $\mu$ mol/L L-glutamine, 100 U/ml penicillin/streptomycin (Life Technologies, Gaithersburg, MD) at 37°C in a 5% CO<sub>2</sub> humidified atmosphere for 18 to 22 hours. Cells were washed twice with prewarmed Hanks' balanced salt solution (HBSS) (Life Technologies), and incubated with 5 mmol/L M $\beta$ CD for 30 minutes or with medium without M $\beta$ CD, as a control group. An additional incubation was performed in the presence of 10 ng/ml of TNF for different times or for 30 minutes at various TNF concentrations. Cells were washed twice with ice-cold PBS, extracted in lysis buffer, and analyzed by SDS-PAGE and immunoblotting for phospho-Akt (Ser473) or for I $\kappa$ B $\alpha$  as described below. To analyze the effects of M $\beta$ CD extraction on cell architecture, EA.hy926 cells were treated with M $\beta$ CD at 5 mmol/L for 30 minutes and then prepared for confocal immunofluorescence or transmission electron microscopy as described above.

### *Isolation of Caveolin-Enriched Membranes*

Purification of caveolae-enriched membrane fractions was performed as described<sup>25</sup> with minor modifications. In brief, EA.hy926 cells were treated with 10 ng/ml of TNF for the indicated time point, washed twice with ice-cold Dulbecco's phosphate-buffered saline, and scraped into 1 ml of 25 mmol/L MES hydrate buffer, pH 6.5, containing 0.15 mol/L NaCl, 5 mmol/L EDTA, and 0.2% Triton X-100 (MBS) with protease inhibitors (10  $\mu$ g/ml aprotinin, 10  $\mu$ g/ml leupeptin, 1 mmol/L sodium orthovanadate, 10 mmol/L NaF, 1 mmol/L Pefabloc) and left 20 minutes on ice. The suspension was subjected to 10 to 15 strokes in a Dounce homogenizer and centrifuged for 10 minutes at 2000 rpm at 4°C to remove nuclei. Clarified postnuclear supernatants were combined with 90% (w/v) sucrose prepared in MBS, transferred to the bottom of a Beckman 12.5-ml ultracentrifuge tubes, and overlaid gently with 6 ml of 35% and 3 ml of 5% sucrose, respectively. The resulting 5 to 40% discontinuous sucrose gradients were centrifuged for 18 to 20 hours at 40,000 rpm in a SW41 Beckman rotor at 4°C to allow the separation of the low-density rafts/caveolae. After centrifugation, a floating light band, corresponding to the Triton X-100 insoluble mate-



rial, was detectable at the interface between 35 and 5% of each gradient. Fractions were harvested from the top to the bottom of the gradients and analyzed either by SDS-PAGE followed by immunoblotting for caveolin-1 or TNFR1 (see below) or for binding of cholera toxin subunit B (CTxB) by dot-blot analysis.

### Immunoblotting and Immunoprecipitation

For immunoblotting experiments, scrape-harvested EA.hy926 cells or isolated cell fractions were extracted in 150  $\mu$ l of lysis buffer (20 mmol/L Tris-HCl, pH 7.5, 150 mmol/L NaCl, 1 mmol/L Na<sub>2</sub>EDTA, 1 mmol/L EGTA, 1% Triton, 2.5 mmol/L sodium pyrophosphate, 1 mmol/L  $\beta$ -glycerophosphate, 1 mmol/L Na<sub>3</sub>VO<sub>4</sub>, 1  $\mu$ g/ml leupeptin, 2% SDS, and 1 mmol/L Pefabloc) for 15 minutes on ice. Lysates were passed several times through a 29-gauge needle to shear DNA in the samples. Unbroken cells and debris were pelleted by centrifugation at 2000 rpm for 10 minutes at 4°C and an equal amount of protein (15  $\mu$ g)-containing supernatant was fractionated by SDS-PAGE,<sup>26</sup> transferred electrophoretically to a nitrocellulose membrane (Trans-Blot transfer medium; Bio-Rad, Hercules, CA), stained with Ponceau S (Sigma), and subjected to immunoblotting with primary antibody followed by incubation with HRP-conjugated secondary antibody. Detection of the bound antibody by enhanced chemiluminescence was performed according to the manufacturer's instructions (Pierce). Results were quantified by densitometric analysis using a computing densitometer (Molecular Dynamics).

For immunoprecipitation experiments, 1200  $\mu$ l total (400  $\mu$ l/sample) from pooled sucrose gradient fractions 3, 4, and 5 or fractions 9, 10, and 11 or unfractionated cell lysates were incubated with 1  $\mu$ g of goat anti-TNFR1 (H5) overnight at 4°C with gentle rocking and immunoprecipitated by adding Protein G-Sepharose (Amersham Biosciences, Piscataway, NJ) for 3 hours at 4°C. Beads were recovered by centrifugation and the samples were eluted by heating washed beads for 3 minutes at 96°C. The eluate was then cleared by centrifugation and immune complexes in the supernatant were subjected to SDS-PAGE and immunoblotting as above.

### Fluorescence Flow Cytometry

For fluorescence flow cytometric analyses, EA.hy926 cells, grown on six-well plates, were treated as indicated with TNF or M $\beta$ CD. At the end of the procedure cells were washed once with ice-cold HBSS and 1% BSA before incubation with biotinylated mouse IgG2a anti-human monoclonal antibody or the appropriate isotype control at 1  $\mu$ g/10<sup>6</sup> cells for 60 minutes on ice. Thereafter, cells were washed twice with HBSS and 1% BSA and incubated 30 minutes at 4°C with streptavidin-phycoerythrin conjugate (Molecular Probes), washed twice in HBSS and 1% BSA, and analyzed with a Beckman FACSsort. Fluorescence of 1.5  $\times$  10<sup>4</sup> cells/sample was acquired and analyzed, using Cellquest software, to quantify the

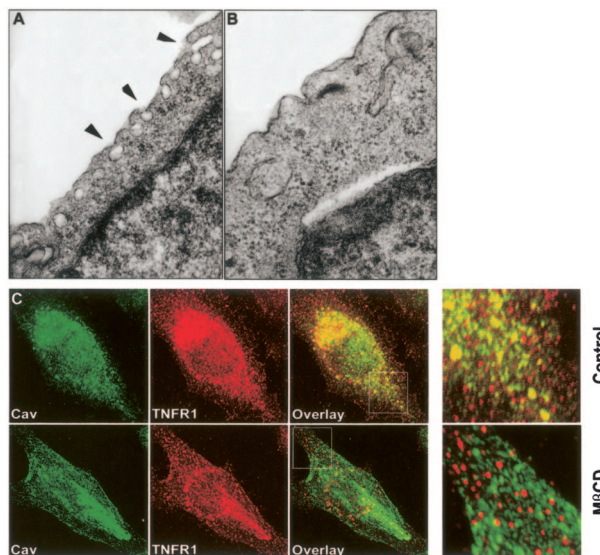


**Figure 1.** Morphological examination of caveolae in resting EA.hy926 cells. **A:** Transmission electron microscopy reveals caveolae, indicated by **arrowheads**, in resting EA.hy926 cells. **B:** EM analysis of M $\beta$ CD-treated cells showing the disappearance of caveolae network. **C:** Confocal immunofluorescence microscopy with a combination of anti-TNFR1/caveolin antibodies in both control (**top**) and M $\beta$ CD-treated (**bottom**) EA.hy926 cells. **White boxes** indicate high magnification (**right**). Note co-localization of TNFR1 and caveolin in the periphery of control but not M $\beta$ CD-treated cells. Data are from two different independent experiments.

surface expression of TNFR1 by calculating the mean fluorescence intensities.

## Results

### Expression of Caveolae and Localization of TNFR1 within the EA.hy926 Cell Line

The human EA.hy926 cell line responds to TNF by expressing E-selectin, an EC-specific response, and has been used for several years as a model for studying EC functions.<sup>27,28</sup> To assess the caveolar system in EA.hy926, we initially used transmission electron microscopy. We observed dense clusters of caveolae close to and in some cases communicating with the cell surface, similar to those displayed by ECs *in situ* (Figure 1A). Incubation of cells with 5 mmol/L M $\beta$ CD, a compound that extracts cholesterol from the plasma membrane induced loss of these organelles, consistent with their identification as caveolae (Figure 1B). These observations suggest that EA.hy926 cells could be suitable for investigating the role(s) of caveolae in TNF signaling in ECs.

To evaluate possible localization of TNFR-1 to caveolae, we first analyzed cells by two-color confocal laser-scanning immunofluorescence microscopy, using caveolin as a marker for caveolae. EA.hy926 cells were grown to confluence, fixed, and stained with a combination of goat anti-TNFR1 and rabbit anti-human caveolin antibodies (Figure 1C, top). Both molecules co-localized to numerous cytosolic granules within the cells, especially in the cell periphery, giving a punctate staining pattern consistent with a caveolar distribution. The same exper-

iment performed after the incubation with 5 mmol/L of M $\beta$ CD for 30 minutes completely abolished the co-localization of TNFR1 with caveolin protein (Figure 1C, bottom). Some TNFR1 and caveolin were also localized to a perinuclear region. By comparing the staining of anti-TNFR1 and anti-Golgin97 by the same technique (data not shown), we confirmed the previous finding made in HUVECs that much of TNFR1 is localized to the Golgi apparatus.<sup>29</sup> However, it is clear that EA.hy926 cells have a substantially larger extra-Golgi pool than do cultured HUVECs, consistent with a generalized collapse of the caveolar network to the Golgi on culture of the latter cell type. A similar redistribution from caveolae to Golgi has been described for the localization of e-NOS in cultured ECs.<sup>30</sup>

### Isolation and Characterization of Caveolae from Resting EA.hy926 Cells

To more definitively establish the caveolar localization of TNFR1 in EA.hy926 cells, we used cell fractionation by sucrose density gradient centrifugation after Dounce homogenization. A sample from each of 11 fractions was adsorbed on a nitrocellulose membrane and stained with HRP-conjugated cholera toxin subunit B (CTxB), a widely used marker for ganglioside G<sub>M1</sub>-containing lipid domains<sup>31–33</sup> such as caveolae.<sup>34–36</sup> This procedure reproducibly (in more than 10 independent experiments) identified a light region cholera toxin-binding membrane population in fractions 3, 4, and 5 (Figure 2A). We next prepared replicate gradients from EA.hy926 cells that were either untreated or subjected to extraction with two concentrations of M $\beta$ CD. In untreated cells (labeled as control), both TNFR1 and caveolin-1 were identified in fractions 3, 4, and 5 by immunoblotting (Figure 2B). Preincubation with 2.5 mmol/L of M $\beta$ CD partially and preincubation with 5 mmol/L M $\beta$ CD strongly decreased the level of both TNFR1 and caveolin-1 in these light fractions (Figure 2B). These observations suggest that the presence of TNFR1 in the light fractions depended on the presence of lipid rafts/caveolae in the cell. Finally, we performed immunoelectron microscopy with both anti-TNFR1 and caveolin antibodies on pooled fractions 3, 4, and 5. This technique showed these fractions to contain caveolae-sized vesicles that stain positively for both TNFR1 and caveolin-1 (Figure 2C). In combination with the confocal immunofluorescence microscopy studies of whole cells described above, these cell fractionation experiments allow us to conclude that plasmalemmal TNFR1 is concentrated within caveolae in human ECs.

### Effects of M $\beta$ CD Disruption of Caveolae on TNF Signaling

To investigate the possible role of caveolae in TNFR1 signaling pathways, we compared the responses of EA.hy926 cells treated with M $\beta$ CD, or not so treated, to addition of TNF. Because the PI3K/Akt pathway is also activated by the presence of factors in serum, EA.hy926

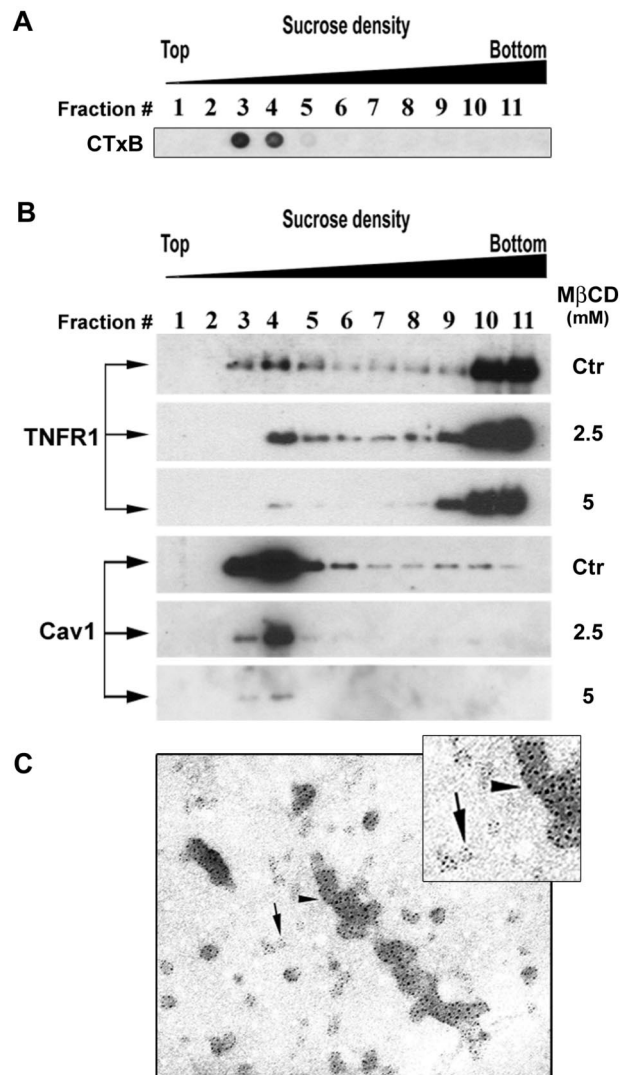


**Figure 2.** Fractionation of EA.hy926 cells on sucrose gradient. **A:** EA.hy926 cells were harvested and fractionated by sucrose density gradient as described in Materials and Methods and 10  $\mu$ l of each sample was subjected to a dot-blot analysis by staining membrane with HRP-conjugated cholera toxin subunit B (CTxB). **B:** EA.hy926 cells were incubated for 30 minutes with two different doses of methyl- $\beta$ -cyclodextrin (M $\beta$ CD) or not treated, Dounce homogenized, and then fractionated by sucrose density gradient. Fractions, harvested from the top to the bottom of each gradient were analyzed by SDS-PAGE and immunoblotted for TNFR1 and caveolin-1. Ctr, indicates control cells not subjected to M $\beta$ CD treatment. **C:** Fractions 3 to 5, pooled after fractionation of resting cells, were subjected to immunoelectron microscopy analysis with both TNFR1 (15 nm, **arrowhead**) and caveolin (5 nm, **arrow**) antibodies. Note co-localization of TNFR1 and caveolae in isolated caveolae.

cells in these experiment were deprived of serum for 22 hours as described in Material and Methods, and then incubated with 5 mmol/L of M $\beta$ CD or left untreated (control) for 30 minutes. Replicate cultures of control or M $\beta$ CD-treated cells were then either treated with 10 ng/ml of TNF for different lengths of time or with different concentrations of TNF for 30 minutes and subjected to SDS-PAGE and immunoblot analysis to assess signaling responses. In both dose-response (Figure 3A) and time-course (Figure 3B) experiments, TNF-induced Akt phosphorylation was strongly inhibited by preincubation with M $\beta$ CD, compared to the control cells (Figure 3B, top).

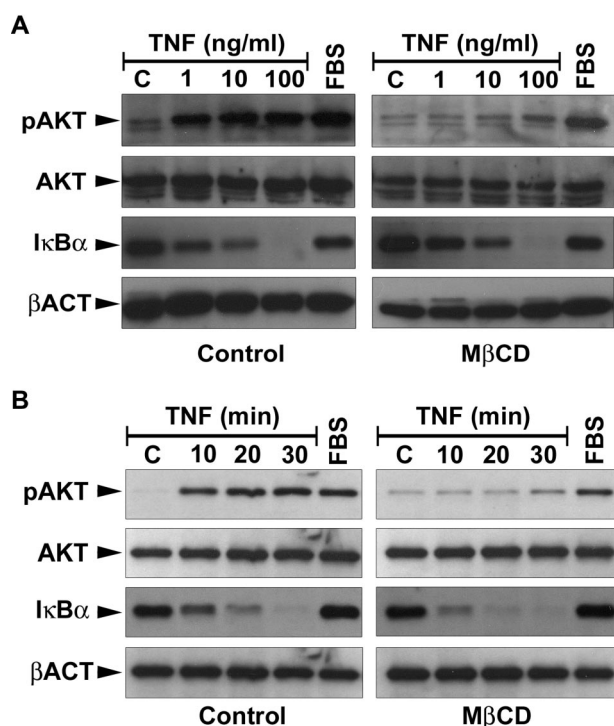


**Figure 3.** Effect of MβCD on TNF responses of EA.hy926 cells. EA.hy926 cells, deprived of serum and growth factor for 18 to 22 hours at 37°C, were pretreated with 5 mmol/L MβCD for 30 minutes at 37°C or left untreated as a control group. Cells were then exposed for 30 minutes to TNF with indicated concentration (**A**) or with 10 ng/ml for the indicated time (**B**) and analyzed by immunoblotting using an antibody specific for both Akt (Ser473), total Akt, or IκBα. fetal bovine serum was used at 10% concentration in both experiments. **Bottom:** The panels show the normalization with β-actin antibody as a test of equal protein loading. Data are from one of three independent experiments with similar results.

However, the phosphorylation of AKT in response to serum (fetal bovine serum) was still intact demonstrating that MβCD treatment did not inhibit all cellular responses of the PI3K system. When we compared the ability of TNF to induce degradation of IκBα in contrast of MβCD-treated cells, no effect was detected, suggesting that MβCD does not modify the NF-κB pathway (Figure 3, A and B). These findings support the interpretation that TNFR1 uses receptor cross talk to activate PI3K but not NF-κB in ECs.

### Effects of TNF on TNFR1 Distribution

TNF has been reported to induce internalization of TNFR1 in the U937 human monocytoid cell line.<sup>37</sup> To examine the effect of TNF on TNFR1 distribution in ECs, we treated EA.hy926 cells with TNF for indicated period of time and then fractionated the cells by sucrose density gradient centrifugation. Aliquots of each fraction for each time point of TNF treatment were first analyzed by immunoblotting for the expression of caveolin-1 (Figure 4A) and TNFR1 (Figure 4B). TNF had no effect on the distribution of caveolin-1 at any time examined. We next examined the same gradients for the distribution of TNFR1. In resting cells, we observed expression of the TNFR1 in the

same fractions that we had found positive for caveolin-1 (Figure 4B). However, treatment with TNF induced a progressive decrease of TNFR1 from caveolin-1-enriched light fractions within the first 5 minutes of stimulation. Densitometric analysis of the TNFR1 and caveolin-1 bands confirmed a significant decrease of TNFR1/caveolin-1 ratio measured in fraction 4 of each time point. (Figure 4C). At the same time, there was no discernable change in levels of TNFR1 in the heavier fractions of the gradient in response to TNF treatment. This suggested that TNF caused disappearance of TNFR1 from the caveolar network. We found no evidence of TNF-induced shedding of TNFR1 into the medium, assayed by enzyme-linked immunosorbent assay, suggesting that receptor was being internalized from caveolae (data not shown). In addition, we performed flow cytometric analysis to evaluate the effect of MβCD on TNF-induced down-regulation of TNFR1 on the cell surface (Figure 4D). TNF induced the down-regulation of TNFR1 in a time-dependent manner, consistent with internalization of receptor. The level of TNFR1 was not affected by extraction of cholesterol with MβCD (Figure 4D, right), suggesting a possible redistribution of receptor to other portions of the plasma membrane as caveolae and other lipid rafts are dissolved. However, MβCD treatment markedly reduced TNF-dependent internalization of TNFR1.

To further characterize the basis of the TNF-induced redistribution of TNFR1, we used the technique of co-immunoprecipitation to look for TNF-induced changes in the interactions of TNFR1 with caveolin-1. We immunoprecipitated TNFR1 from a total lysate prepared with resting cells and immunoblotted for TNFR1 or caveolin-1. This experiment showed the interaction of the receptor with caveolin-1 (Figure 5, R). Preincubation with MβCD for 30 minutes disrupted this interaction. We then pooled the caveolin-1-enriched light fractions (3 to 5) as well as denser membrane fractions (9 to 11) from untreated and TNF-treated EA.hy926 cells, prepared a detergent lysate, and immunoprecipitated these fractions with TNFR1 antibody. The resulting immunoprecipitates were similarly immunoblotted for TNFR1 and for caveolin-1 (Figure 5, right). In resting cells, caveolin-1 co-immunoprecipitated with TNFR1 from the caveolar fraction but not from the dense membrane fraction. Incubation with 10 ng/ml of TNF induced dissociation between the two molecules in the caveolae-enriched light fractions starting from 5 minutes. Although some expression of TNFR1 was still detectable in caveolae after 15 minutes, it was no longer associated with caveolin-1. The denser fractions failed to show association of TNFR1 with caveolin-1 even after TNF treatment. These findings suggest that TNF induces dissociation of its own receptor from caveolin-1, probably within caveolae, raising a possible role for this organelle as the site of receptor internalization. Our findings also suggest that the interaction between TNFR1 and caveolin-1 occurs only within the caveolar network. Interestingly, we detected the reappearance of TNFR1 in caveolin-1-enriched fractions again at 60 and 240 minutes after TNF stimulation, and the receptor once again could be co-immunoprecipitated with caveolin-1 (Figure 5). This reappearance of TNFR1 in the caveolae and its reasso-



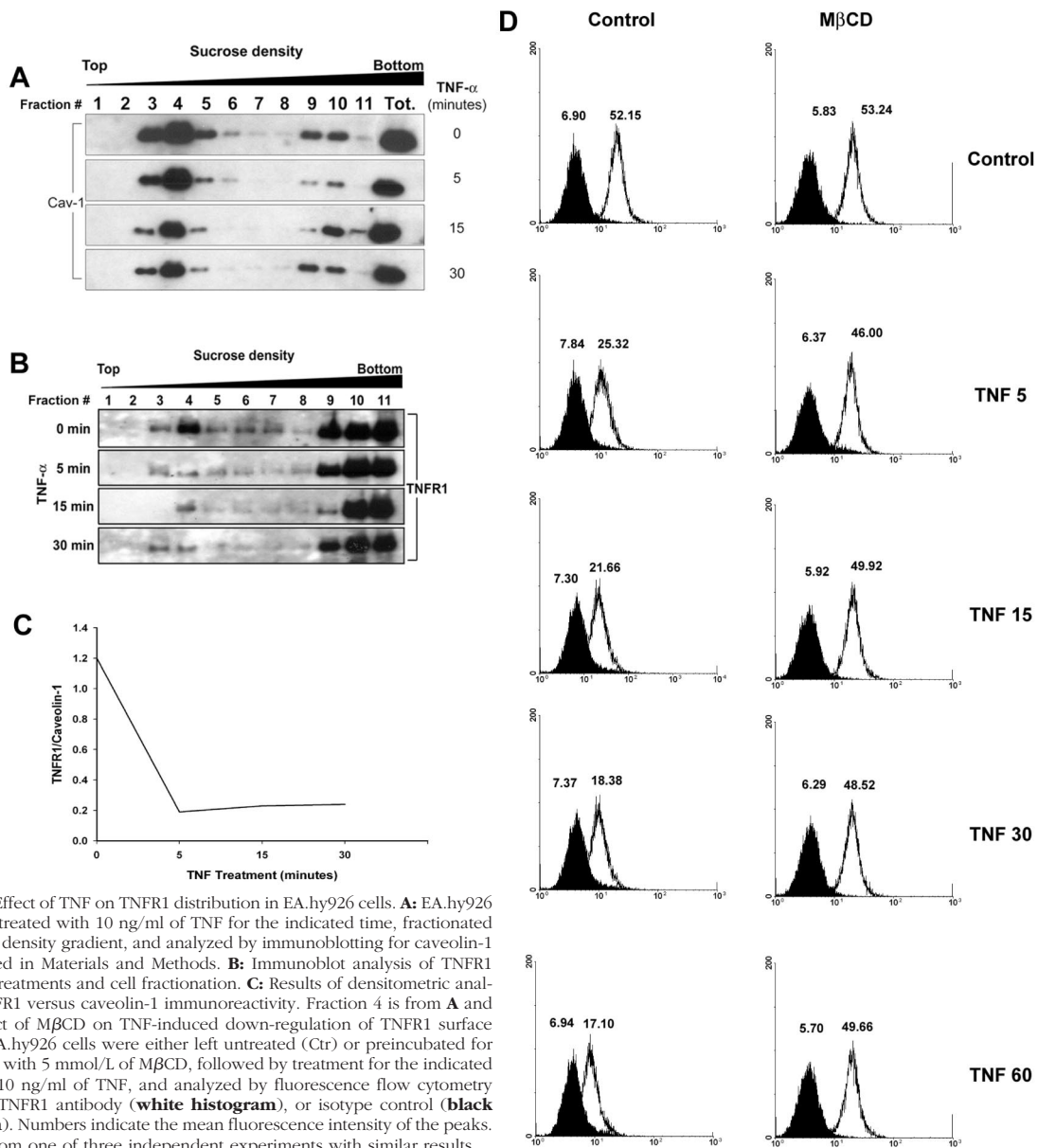


**Figure 4.** Effect of TNF on TNFR1 distribution in EA.hy926 cells. **A:** EA.hy926 cells were treated with 10 ng/ml of TNF for the indicated time, fractionated by sucrose density gradient, and analyzed by immunoblotting for caveolin-1 as described in Materials and Methods. **B:** Immunoblot analysis of TNFR1 after TNF treatments and cell fractionation. **C:** Results of densitometric analysis of TNFR1 versus caveolin-1 immunoreactivity. Fraction 4 is from **A** and **B**. **D:** Effect of M $\beta$ CD on TNF-induced down-regulation of TNFR1 surface staining. EA.hy926 cells were either left untreated (Ctr) or preincubated for 30 minutes with 5 mmol/L of M $\beta$ CD, followed by treatment for the indicated time with 10 ng/ml of TNF, and analyzed by fluorescence flow cytometry using anti-TNFR1 antibody (white histogram), or isotype control (black histogram). Numbers indicate the mean fluorescence intensity of the peaks. Data are from one of three independent experiments with similar results.

ciation with caveolin-1 could be because of new receptor synthesis, to recycling of internalized receptor, or replacement of internalized receptors from stored receptors within the Golgi apparatus.

To investigate the fate of TNFR1 molecules that exit the caveolae in response to ligand binding, we performed time-course experiments by using two-color confocal scanning laser immunofluorescence microscopy and antibodies for receptor as well as for different intracellular compartments. In EA.hy926 cells, as in most other cell types, the majority of TNFR1 molecules are found in the Golgi. However, it is possible to draw some inference about the internalization by focusing on the minority population of receptor found in the cell periphery. Many receptors are internalized via a coated pit/coated vesicle pathway. The protein coating on the cytosolic face of these organelles is formed predominantly by clathrin. To determine whether this system participated in ligand-

induced internalization of TNFR1, we examined EA.hy926 cells for co-localization of TNFR1 and clathrin. We did not observe coincidence of these molecules in resting cell or in TNF-treated cells in the region of the cell surface at any time point examined. This contrasts with the behavior of transferrin receptor, which, as expected, does co-localize with clathrin. We did observe co-localization of TNFR1 and clathrin in the Golgi region, but this did not change with TNF treatment (Figure 6). We also did not observe co-localization of TNFR1 with mitochondria (data not shown), which are a repository for internalized TNF molecules.<sup>38</sup> However, using antibodies to both EEA1 and Rab5, two different markers for endosomes, we found that TNF causes trafficking of TNFR1 to the endosomal pathway within 60 minutes (Figure 7, A and B). These findings suggest that TNF induces trafficking of its own receptor from caveolae to the endosomal pathway, independent of clathrin-coated pits. We do not know if endo-

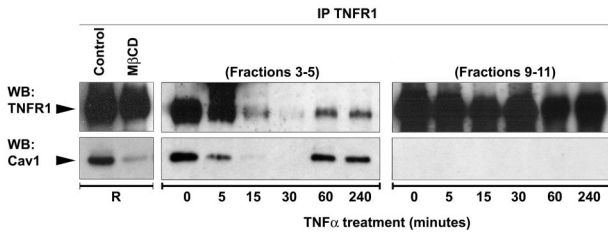


**Figure 5.** Co-immunoprecipitation of TNFR1 and caveolin-1 from caveolae in EA.hy926 cells. EA.hy926 cells were stimulated with TNF for the indicated time and fractionated by sucrose gradient as described in Materials and Methods. Four hundred  $\mu$ l from fractions 3, 4, and 5 (left), and from 9, 10, and 11 were mixed and immunoprecipitated with TNFR1 followed by SDS-PAGE analysis with both TNFR1 and caveolin-1 antibodies. Note that although both the proteins are represented in fractions 9 to 11 (see Figure 4A), no interaction between the two proteins was detected. Immunoprecipitation of TNFR1 performed in resting cells not subjected to the fractionation procedure, shows the ability of M $\beta$ CD to disrupt the association between TNFR1 and caveolin-1, as indicated by R at the left. Data are from one of three independent experiments with similar results.

somes play a role in TNF signaling or in termination of TNF signaling.

**Discussion**

In this report we show that EA.hy926, a cell line produced by fusing HUVECs with the permanent human lung carcinoma cell line A549, not only recapitulates EC-like responses to TNF, such as E-selectin induction, but also retains an extensive caveolar network, unlike HUVECs that lose these organelles when allowed to grow in cul-

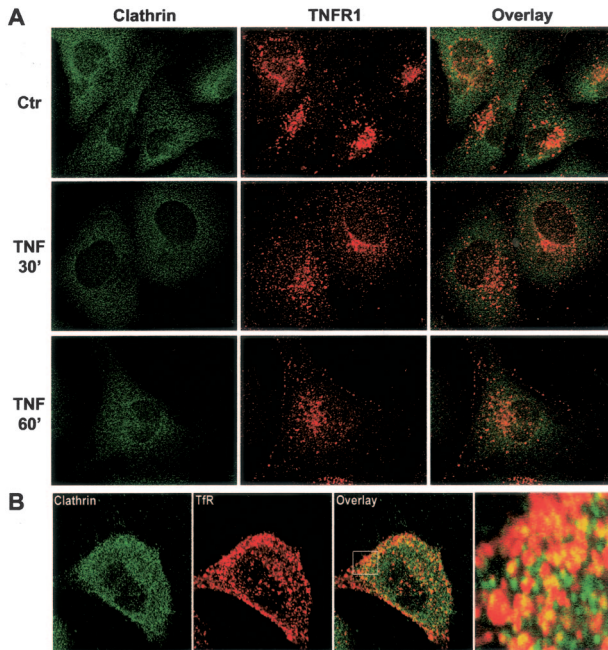


**Figure 6.** TNFR1 does not internalize in clathrin-coated structures in EA.hy926 cells. **A:** EA.hy926 cells were either left untreated or treated for different periods of time with 10 ng/ml of TNF as indicated and analyzed by laser confocal microscopy after immunostaining with a combination of goat anti-human TNFR1 and mouse anti-clathrin heavy chain antibodies. **B:** Confocal analysis of clathrin and transferrin receptor (TTR) in resting EA.hy926 cells. **Right:** Higher magnification (indicated by box) of the overlay image. Images shown are representative of three independent experiments with similar results. Original magnifications,  $\times 63$ .

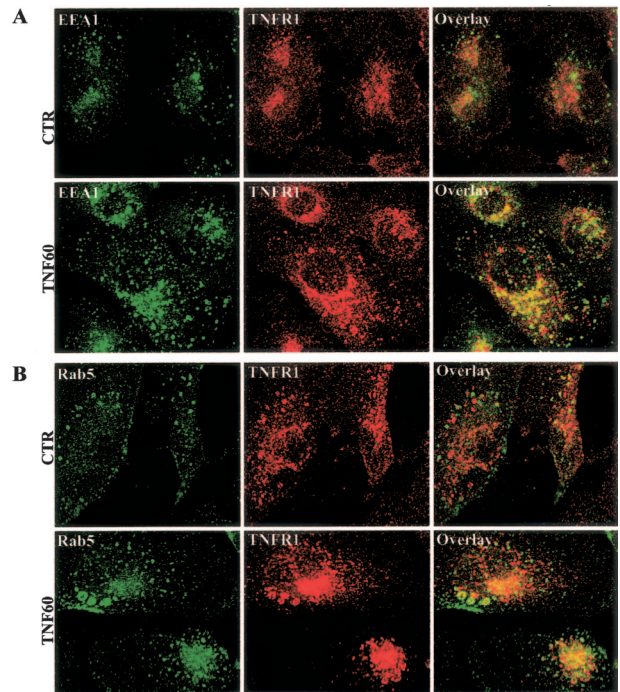


**Figure 7.** TNF-induced trafficking of TNFR1 to endosomes in EA.hy926 cells. EA.hy926 cells were treated with 10 ng/ml of TNF and subjected to confocal fluorescent microscopy by staining with a combination of TNFR1 with either EEA1 (A) or Rab5 (B) antibodies. Images shown are from one of three different experiments with similar results.

ture. EA.hy926 cells thus offer an opportunity to investigate the functions that caveolae may play in various TNF responses of ECs. We make three new observations using this model system. First, in resting ECs, TNFR1 associates with caveolin-1 and is localized to caveolae. Second, disruption of caveolae (and other lipid rafts) selectively inhibits the activation of the PI3K/Akt pathway, and not the NF- $\kappa$ B pathway, consistent with a mechanism in which TNFR1 activates PI3K via receptor cross talk. The other receptors and adaptors involved in this pathway are yet to be determined. And third, we find that TNF causes rapid internalization of TNFR1 from caveolae, resulting in receptor accumulation in endosomes without apparent involvement of a clathrin-coated pit/coated vesicle uptake mechanism.

Caveolin-1 has been previously found associated with TRAF2 but not with TNFR1, TNFR2, or TRADD in resting HUVECs.<sup>39</sup> A key difference from these earlier studies is that HUVECs, despite retaining expression of caveolin-1 and -2, no longer form caveolae. This may explain why the interaction of TNFR1 and caveolin-1 may be observed in EA.hy926 cells but not in HUVECs. This difference also raises the possibility that the interaction of caveolin-1 with TNFR1 is not direct, but depends on the presence of some additional protein found in caveolae. It has been suggested that the death domain of TNFR1 may play an important role to promote the appropriate localization of the receptor to caveolae.<sup>40</sup> We do not yet know if this region of TNFR1 is also involved in the interaction with caveolin-1. We also do not yet know which motif within caveolin-1 is involved in the interaction with TNFR1.



The role of lipid rafts in the PI3K/PKB pathway has been extensively studied. A plasma membrane raft-associated PKB Ser473 kinase has been recently discovered<sup>41</sup> and its function is sensitive to drugs able to disrupt rafts from the plasma membrane. In addition, EGFR, a receptor that activates an anti-apoptotic PI3K/Akt signaling pathway, has been shown to be unable to protect cells from apoptosis when they were preincubated with filipin, similar to the results generated using the PI3K inhibitor LY294002.<sup>42</sup> In this report we demonstrate that disrupting caveolae by extracting cholesterol from the plasma membrane by using M $\beta$ CD strongly impairs TNF-mediated phosphorylation of Akt at Ser473, but not TNF-induced I $\kappa$ B $\alpha$  degradation, consistent with the involvement of cholesterol-enriched raft domains in the regulation of PI3K pathway.<sup>15</sup> A cross-talk model between TNFR2 and VEGFR2 has been recently proposed.<sup>22</sup> According to this model, TNF induces transactivation of VEGFR2 via Etk, by phosphorylating the receptor at a subset of the sites that are phosphorylated in response to VEGF, leading to the activation of PI3K/Akt but not of PLC- $\gamma$ . This precise mechanism is probably not involved in our studies of EA.hy926 cells because no interactions between TNFR1 and Etk have been demonstrated. It is formally possible that TNF activation of PI3K in EA.hy926 cells is in part mediated by TNFR2, but pilot experiments with antagonistic anti-TNFR1 antibody and with a selective TNFR1-binding mutant of TNF show clear evidence of involvement of TNFR1 in the PI3K response of EA.hy926 cells, similar to published results with HUVECs (A. D'Alessio and J.S. Pober, unpublished observation).<sup>17</sup> An alternative cross-talk pathway could arise from TNF-induced synthesis of sphingosine 1-phosphate, a lipid mediator that could activate PI3K via a G protein-coupled Edg receptor.<sup>43</sup>

An important issue raised by our study is the relationship between caveolae and lipid rafts in ECs. Cultured ECs lose their caveolae, and it is likely that as caveolae disassemble, the lipid component remains organized as rafts. Rafts are likely to retain the ability to promote receptor cross talk and we have seen that M $\beta$ CD treatment effectively inhibits TNF activation of Akt in HUVECs (A. D'Alessio and J.S. Pober, unpublished observation).

The ability of TNF to induce internalization of TNFR1 from the cell surface has been previously described in the U937 human monocytoid cell line,<sup>37</sup> but we had not been able to confirm such a response in cultured HUVECs,<sup>29</sup> probably because so few TNFR1 molecules are expressed on the cell surface once the caveolar network collapses. However, as reported here, TNF does cause disappearance of TNFR1 from the cell surface of EA.hy926 cells, as detected by fluorescence flow cytometry, and from caveolae, as detected by cell fractionation. Because TNF does not induce receptor shedding, we interpret this as evidence of ligand-induced TNFR1 internalization from caveolae. The fact that the level of TNFR1 detected on the cell surface does not change after cholesterol extraction implies that M $\beta$ CD induces a redistribution of the receptor from caveolae to other parts of the cell surface. It is theoretically possible that TNF-induced dissociation of TNFR1 from caveolin-1 starts with a similar

migration of receptor to plasmalemmal regions outside of the caveolae followed by internalization via clathrin-coated pits. This seems unlikely on two grounds, namely the rapidity of the internalization and from our failure to see TNFR1 in clathrin-coated pits or vesicles. The likeliest interpretation of our findings is that TNFR1 is directly internalized from caveolae. This is consistent with several recent studies that have described an internalization mechanism directly initiated from caveolae.<sup>44</sup> Although the caveolar uptake mechanism is primarily used by viral proteins or GPI-linked membrane proteins, it has been recently demonstrated that transforming growth factor- $\beta$  receptors can be internalized either by clathrin-vesicles in or by lipid raft-dependent pathway,<sup>45</sup> suggesting that pathway may also be used to internalize conventional transmembrane proteins such as TNFR1.

In summary, we have demonstrated that TNFR1 is concentrated within the caveolae of a human EC line and that interfering with caveolae organization by extracting cholesterol abolishes the ability of TNF to activate Akt. In contrast to some previous reports,<sup>15</sup> we have not found an effect of this manipulation on the activation of NF- $\kappa$ B, consistent with our previous finding that in ECs, unlike certain other cell types, the PI3K/Akt pathway is not involved in activation of NF- $\kappa$ B.<sup>17</sup> In addition, we have observed a direct interaction between TNFR1 and caveolin-1 within caveolae that may function to retain TNFR1 within the caveolar network, and that ligand binding induces a rapid dissociation of this complex, initiating internalization of the receptor directly from caveolae. The broader implication of these studies is that caveolae could play a major role in TNF responses of vascular ECs that, because of loss of caveolae in cell culture, has been unappreciated in previous investigations.

## Acknowledgments

We thank Dr. Fulvio D'Acquisto for helpful discussion and critical suggestions about the caveolae isolation protocol and Dr. William Sessa for helpful discussion and provision of the EA.hy926 cell line.

## References

1. Vassalli P: The pathophysiology of tumor necrosis factors. *Annu Rev Immunol* 1992, 10:411–452
2. Fiers W: Tumor necrosis factor. Characterization at the molecular, cellular and in vivo level. *FEBS Lett* 1991, 285:199–212
3. Locksley RM, Killeen N, Lenardo MJ: The TNF and TNF receptor superfamilies: integrating mammalian biology. *Cell* 2001, 104:487–501
4. Ledgerwood EC, Pober JS, Bradley JR: Recent advances in the molecular basis of TNF signal transduction. *Lab Invest* 1999, 79:1041–1050
5. Al-Lamki RS, Wang J, Skepper JN, Thiru S, Pober JS, Bradley JR: Expression of tumor necrosis factor receptors in normal kidney and rejecting renal transplants. *Lab Invest* 2001, 81:1503–1515
6. Jones SJ, Ledgerwood EC, Prins JB, Galbraith J, Johnson DR, Pober JS, Bradley JR: TNF recruits TRADD to the plasma membrane but not the trans-Golgi network, the principal subcellular location of TNF-R1. *J Immunol* 1999, 162:1042–1048
7. Bradley JR, Johnson DR, Pober JS: Four different classes of inhibitors of receptor-mediated endocytosis decrease tumor necrosis factor-

- induced gene expression in human endothelial cells. *J Immunol* 1993, 150:5544–5555
8. Schutze S, Machleidt T, Adam D, Schwandner R, Wiegmann K, Kruse ML, Heinrich M, Wickel M, Kronke M: Inhibition of receptor internalization by monodansylcadaverine selectively blocks p55 tumor necrosis factor receptor death domain signaling. *J Biol Chem* 1999, 274:10203–10212
  9. Helms JB, Zurzolo C: Lipids as targeting signals: lipid rafts and intracellular trafficking. *Traffic* 2004, 5:247–254
  10. Palade GE: Fine structure of blood capillaries. *J Appl Physiol* 1953; 24:1424–1436
  11. Yamada E: The fine structure of the gall bladder epithelium of the mouse. *J Biophys Biochem Cytol* 1955, 1:445–458
  12. Razani B, Woodman SE, Lisanti MP: Caveolae: from cell biology to animal physiology. *Pharmacol Rev* 2002, 54:431–467
  13. Lisanti MP, Scherer PE, Tang Z, Sargiacomo M: Caveolae, caveolin and caveolin-rich membrane domains: a signalling hypothesis. *Trends Cell Biol* 1994, 4:231–235
  14. Ko YG, Lee JS, Kang YS, Ahn JH, Seo JS: TNF-alpha-mediated apoptosis is initiated in caveolae-like domains. *J Immunol* 1999, 162:7217–7223
  15. Legler DF, Micheau O, Doucey MA, Tschopp J, Bron C: Recruitment of TNF receptor 1 to lipid rafts is essential for TNF-alpha-mediated NF-kappaB activation. *Immunity* 2003, 18:655–664
  16. Burow ME, Weldon CB, Melnik LI, Duong BN, Collins-Burrow BM, Beckman BS, McLachlan JA: PI3-K/AKT regulation of NF-kappaB signaling events in suppression of TNF-induced apoptosis. *Biochem Biophys Res Commun* 2000, 271:342–345
  17. Madge LA, Pober JS: A phosphatidylinositol 3-kinase/Akt pathway, activated by tumor necrosis factor or interleukin-1, inhibits apoptosis but does not activate NF-kappaB in human endothelial cells. *J Biol Chem* 2000, 275:15458–15465
  18. Osawa Y, Banno Y, Nagaki M, Brenner DA, Naiki T, Nozawa Y, Nakashima S, Moriwaki H: TNF-alpha-induced sphingosine 1-phosphate inhibits apoptosis through a phosphatidylinositol 3-kinase/Akt pathway in human hepatocytes. *J Immunol* 2001, 167:173–180
  19. Osawa Y, Nagaki M, Banno Y, Brenner DA, Asano T, Nozawa Y, Moriwaki H, Nakashima S: Tumor necrosis factor alpha-induced interleukin-8 production via NF-kappaB and phosphatidylinositol 3-kinase/Akt pathways inhibits cell apoptosis in human hepatocytes. *Infect Immun* 2002, 70:6294–6301
  20. Gustin JA, Ozes ON, Akca H, Pincheira R, Mayo LD, Li Q, Guzman JR, Korgaonkar CK, Donner DB: Cell type-specific expression of the I-kappaB kinases determines the significance of phosphatidylinositol 3-kinase/Akt signaling to NF-kappa B activation. *J Biol Chem* 2004, 279:1615–1620
  21. Ozes ON, Mayo LD, Gustin JA, Pfeffer SR, Pfeffer LM, Donner DB: NF-kappaB activation by tumour necrosis factor requires the Akt serine-threonine kinase. *Nature* 1999, 401:82–85
  22. Zhang R, Xu Y, Ekman N, Wu Z, Wu J, Alitalo K, Min W: Etk/Bmx transactivates vascular endothelial growth factor 2 and recruits phosphatidylinositol 3-kinase to mediate the tumor necrosis factor-induced angiogenic pathway. *J Biol Chem* 2003, 278:51267–51276
  23. Vasile E, Qu H, Dvorak HF, Dvorak AM: Caveolae and vesiculo-vacuolar organelles in bovine capillary endothelial cells cultured with VPF/VEGF on floating Matrigel-collagen gels. *J Histochem Cytochem* 1999, 47:159–167
  24. Edgell CJ, McDonald CC, Graham JB: Permanent cell line expressing human factor VIII-related antigen established by hybridization. *Proc Natl Acad Sci USA* 1983, 80:3734–3737
  25. Sargiacomo M, Sudol M, Tang Z, Lisanti MP: Signal transducing molecules and glycosyl-phosphatidylinositol-linked proteins form a caveolin-rich insoluble complex in MDCK cells. *J Cell Biol* 1993, 122:789–807
  26. Laemmli UK: Cleavage of structural proteins during the assembly of the head of bacteriophage T4. *Nature* 1970, 227:680–685
  27. Laegreid A, Medvedev A, Nonstad U, Bombara MP, Ranges G, Sundan A, Espevik T: Tumor necrosis factor receptor p75 mediates cell-specific activation of nuclear factor kappa B and induction of human cytomegalovirus enhancer. *J Biol Chem* 1994, 269:7785–7791
  28. Burke-Gaffney A, Hellewell PG: Tumour necrosis factor-alpha-induced ICAM-1 expression in human vascular endothelial and lung epithelial cells: modulation by tyrosine kinase inhibitors. *Br J Pharmacol* 1996, 119:1149–1158
  29. Bradley JR, Thiru S, Pober JS: Disparate localization of 55-kd and 75-kd tumor necrosis factor receptors in human endothelial cells. *Am J Pathol* 1995, 146:27–32
  30. Garcia-Cardena G, Oh P, Liu J, Schnitzer JE, Sessa WC: Targeting of nitric oxide synthase to endothelial cell caveolae via palmitoylation: implications for nitric oxide signaling. *Proc Natl Acad Sci USA* 1996, 93:6448–6453
  31. Janes PW, Ley SC, Magee AI: Aggregation of lipid rafts accompanies signaling via the T cell antigen receptor. *J Cell Biol* 1999, 147:447–461
  32. Parton RG: Ultrastructural localization of gangliosides; GM1 is concentrated in caveolae. *J Histochem Cytochem* 1994, 42:155–166
  33. Harder T, Scheiffele P, Verkade P, Simons K: Lipid domain structure of the plasma membrane revealed by patching of membrane components. *J Cell Biol* 1998, 141:929–942
  34. Lencer WI, Hirst TR, Holmes RK: Membrane traffic and the cellular uptake of cholera toxin. *Biochim Biophys Acta* 1999, 1450:177–190
  35. Montesano R, Roth J, Robert A, Orci L: Non-coated membrane invaginations are involved in binding and internalization of cholera and tetanus toxins. *Nature* 1982, 296:651–653
  36. Orlandi PA, Fishman PH: Filipin-dependent inhibition of cholera toxin: evidence for toxin internalization and activation through caveolae-like domains. *J Cell Biol* 1998, 141:905–915
  37. Higuchi M, Aggarwal BB: TNF induces internalization of the p60 receptor and shedding of the p80 receptor. *J Immunol* 1994, 152:3550–3558
  38. Ledgerwood EC, Prins JB, Bright NA, Johnson DR, Wolfreys K, Pober JS, O'Rahilly S, Bradley JR: Tumor necrosis factor is delivered to mitochondria where a tumor necrosis factor-binding protein is localized. *Lab Invest* 1998, 78:1583–1589
  39. Feng X, Gaeta ML, Madge LA, Yang JH, Bradley JR, Pober JS: Caveolin-1 associates with TRAF2 to form a complex that is recruited to tumor necrosis factor receptors. *J Biol Chem* 2001, 276:8341–8349
  40. Cottin V, Doan JE, Riches DW: Restricted localization of the TNF receptor CD120a to lipid rafts: a novel role for the death domain. *J Immunol* 2002, 168:4095–4102
  41. Hill MM, Feng J, Hemmings BA: Identification of a plasma membrane Raft-associated PKB Ser473 kinase activity that is distinct from ILK and PDK1. *Curr Biol* 2002, 12:1251–1255
  42. Zhuang L, Lin J, Lu ML, Solomon KR, Freeman MR: Cholesterol-rich lipid rafts mediate akt-regulated survival in prostate cancer cells. *Cancer Res* 2002, 62:2227–2231
  43. Morales-Ruiz M, Lee MJ, Zollner S, Gratton JP, Scotland R, Shiojima I, Walsh K, Hla T, Sessa WC: Sphingosine 1-phosphate activates Akt, nitric oxide production, and chemotaxis through a Gi protein/phosphoinositide 3-kinase pathway in endothelial cells. *J Biol Chem* 2001, 276:19672–19677
  44. Pelkmans L, Helenius A: Endocytosis via caveolae. *Traffic* 2002, 3:311–320
  45. Di Guglielmo GM, Le Roy C, Goodfellow AF, Wrana JL: Distinct endocytic pathways regulate TGF-beta receptor signalling and turnover. *Nat Cell Biol* 2003, 5:410–421